Ab-initio Powder Structure Determination of Dichloro[1,2-ethanediylbis(iminomethylene)bis(phosphonato)]trizinc Dihydrate

Naima Bestaoui,[a] Ekaterina V. Bakhmutova-Albert,[a] Ana Vega Rodriguez,[b] Ricardo Llavona,[b] and Abraham Clearfield*[a]

Keywords: Metal phoshonates / Zinc

The reaction of zinc chloride with 1,2-ethanediylbis(iminomethylene)bis(phosphonic acid) in acidic conditions yielded dichloro[1,2-ethanediylbis(iminomethylene)bis(phosphonato)]trizinc dihydrate, $Zn_3Cl_2(HO_3PCH_2NHCH_2CH_2NHCH_2PO_3H)_2{\cdot}2H_2O$ which crystallizes in the monoclinic system and space group $P2_1/n$, with the unit cell parameters a = 9.94316(4), b = 10.44577(5), c = 24.3240(1) Å, β = 90.003(1)°, and Z = 4. The crystal structure was determined ab initio from its powder pattern using the programs EXPO and GSAS. The zinc atoms are in tetrahedral environment and form 16-membered rings with the phosphonate groups. The structure is clearly different from that of the corresponding Cd complex in that the Cd is sixfold coordinated and of different ligand to metal ratio.

Introduction

A major effort has been devoted in our laboratory towards the synthesis and characterization of metal phosphonates.[1] Notable studies in this area of research have also been carried out by Alberti et al.,[2] Bujoli and coworkers[3] and in Ferey's laboratory.[4] One general ligand type that we utilized is the α,ω-alkyldiphosphonic acid. These acids formed semi-crystalline products of the general formula $Zr[O_3P(CH_2)_nPO_3]$ with group 4 metals whose morphology and X-ray powder patterns indicate layered structures in which the layers are cross-linked by the alkyl groups.[5] Similar compounds were prepared using Zn and Cu as the metals.[6,7] These latter compounds were sufficiently crystalline that their structures could be determined from X-ray powder data. Indeed the copper structures confirmed the layered nature of the compounds and in these compounds the alkyl chains are perpendicular to the layers.

Interlayer spacings of the zirconium alkylene derivatives indicated that the chains are inclined at about 60° to the mean plane of the layers and that the layer structures differ from those of the transition metal compounds. Subsequently, zirconium diphosphonic acid derivatives in which the alkyl chains contained amino groups were prepared. Although the compounds were amorphous, they exhibited anion exchange and complexing behavior.[8]

Divalent metals often form crystalline phosphonates; it was of interest to prepare cross-linked layered derivatives containing the amino functionality. Determination of such structures would provide a model for understanding the ion exchange and complexation reactions via structural data. In this paper we report the structure of a chloro(ethylenediaminediphosphonato)zinc. The ligand employed was $H_2O_3PCH_2NHCH_2CH_2NHCH_2PO_3H_2$ (H_4L) which exists in solution as a di-zwitterion. In a previous paper[9] we described the synthesis and characterization of chloro(amino)-(phosphonato) cadmium which crystallizes in a monoclinic system and has a layered type structure, the layers being held together by hydrogen bonding. In the cadmium compound the Cd atoms form dimers through bridging chlorides. These dimers are in turn formed into rows by the phosphonate groups and the rows are crosslinked by the organic chain of the ligand into layers.

In this paper, we are presenting the interaction of the same ligand with zinc chloride in an acidic medium. This led to the formation of $Zn_3Cl_2(H_2L)_2{\cdot}2H_2O$, whose structure, quite different from the previous cadmium structure,[9] is presented here as characterized by its X-ray structure derived from powder data and FTIR.

Results and Discussion

Thermogravimetric Studies: The TGA diagram of $Zn_3Cl_2(H_2O)_2(H_2L)_2$, presented in Figure 1, shows three weight losses. The first step begins at 100 °C and indicates the release of two water molecules by 195 °C. The observed weight loss (4.15%) is in agreement with the calculated value (4.53%). The temperature of dehydration indicates that molecules of water are either coordinated with the zinc atom or strongly hydrogen-bonded. The next process is the

[a] Department of Chemistry, Texas A&M University, College Station, Texas 77843-3255, USA
[b] Departamento de Quimica Organica e Inorganica, Universidad de Oviedo, 33071 Oviedo, Spain

 DOI: 10.1002/ejic.200400878

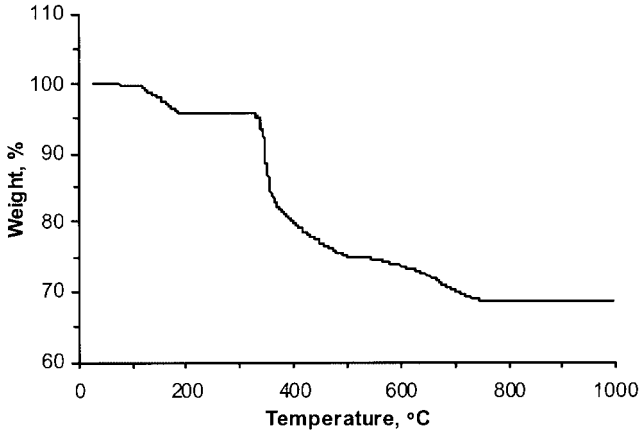

Figure 1. TGA curve for $Zn_3Cl_2L_2{\cdot}2H_2O$.

decomposition of the organic moieties and phosphonic groups accompanied by the formation of oxychloro derivatives, which begins at 350 °C. The process is completed at 758 °C with the formation of a final residue of 68.93%. The product can be formulated as a 1:1 mixture of $Zn(PO_3)_2$/$Zn_2P_2O_7$ (calcd. residue 66.40%). The total weight loss is 31.07% as compared to the calculated value of 33.43% based on the ideal formula.

Description of the Structure

The structure contains three crystallographic independent Zn atoms; they are all in a tetrahedral environment. Zn1 and Zn3 are both bonded to four oxygen atoms from the phosphonate groups. The Zn–O distances vary between 1.957(8) Å and 2.003(8) Å, and are in the order of a normal Zn–O bond. Zn2 is different as it is connected to two oxygen atoms from the phosphonate groups at distances of 1.967(9) and 2.020(9) Å and two chlorine atoms [2.254(8) Å and 2.379(8) Å].

The four phosphorus atoms are in tetrahedral environments consisting of three oxygen atoms and one carbon atom, divided into two distinct groups. In group P1 and P2, the three oxygen atoms bond to each of the three Zn atoms; in this case the order of the P–O bond is between 1.508(8) and 1.531(9) Å. In the P3 and P4 group, only two of their oxygen atoms each bond to Zn1 and Zn3. In this case the non-bonded oxygen atoms O8 and O11 are located at respective distances of 1.542(9) and 1.533(9) Å. These distances are slightly longer than the bonded P–O distance but similar considering the large e.s.d. values.

Zn1 and Zn3 are connected to each other through O–P–O bridging in both the *a*- and *b*-axis directions. Along the *a*-axis the bridging is by alternating P3 and P4 phosphonate groups and in the *b*-axis direction by P1 and P2 groups (Figure 2). This connectivity results in 16-membered rings (counting all the ring atoms). The Zn2 atoms lie in rows parallel to the *b*-axis sandwiched between the Zn1, Zn3 rows as seen in Figure 3. In the *c*-axis direction, the *z* parameter of the Zn2 atoms is very nearly 0,1/2 (Figure 3). This siting places them at intervals of every two rows of Zn1 and Zn3. The coordination of Zn2 is also tetrahedral but from both chloride ions and O4 from P1 and O6 from P2. The linkage in the *c*-axis direction is to form two sets of 16-membered rings, one involving Zn1 and Zn3 and the other with Zn3 and Zn2 alternating with Zn1, Zn2. The carbon−nitrogen chains criss-cross each other connecting P1 bonded to three Zn atoms to P4 bonded to Zn1 and Zn3 (Figure 4). Similarly, P2 bonds to three Zn atoms and P3 to two forming a three dimensional structure.

The localization of the hydrogen atoms allowed us to characterize the hydrogen bonding in the structure and led us to a better understanding of the structure. The structure show an extensive hydrogen bond network going from the chlorine atoms to the two water molecules, to the nitrogen atoms and to the non-metal-bonded oxygen atoms in phosphonate groups P3–O8 and P4–O11. There are four different nitrogen atoms. The C1–N1–C2 angle is 107.7(6)°

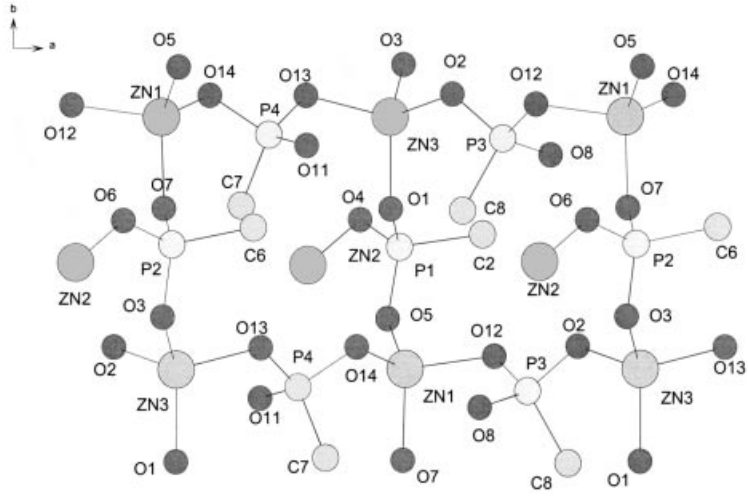

Figure 2. Connectivity of the zinc atoms in the *a*,*b* plane. Zn1 and Zn3 are four coordinates and connected to phosphonate oxygen atoms forming a 16-membered rings.

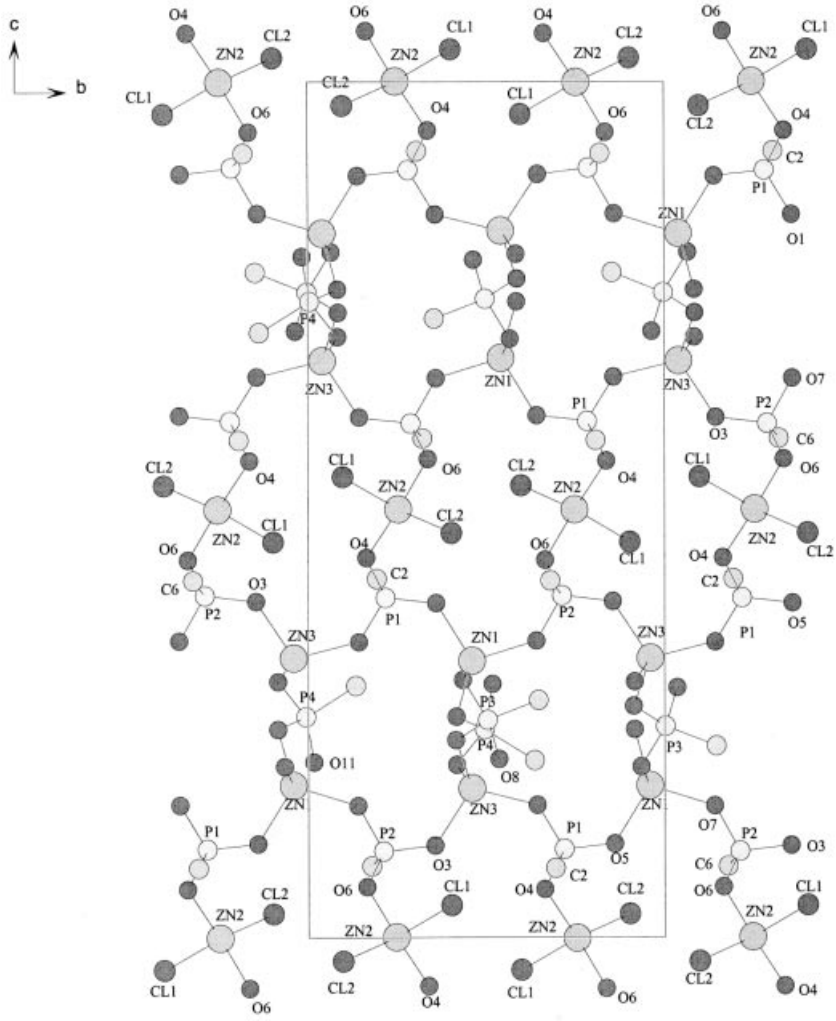

Figure 3. Connectivity of the zinc atoms in the *b*,*c* plane. Zn1, Zn2 and Zn3 are four coordinates and connected to phosphonate oxygen atoms forming a 16-membered rings.

close to the tetrahedral angle of 109°; two hydrogen atoms are located on this nitrogen atom. This shows its tetrahedral symmetry and protonated nature. This atom is hydrogen-bonded to O8 (the free oxygen from P3) through H21. The distance N1···O8 is 2.81 Å on the order of a hydrogen bond length, the bond angle N1–H21···O8 is 130.9° and the distance H21···O8 is 2.04 Å. We could not find any hydrogen atom bonded to O8, therefore O8 is negatively charged. However O8 is also hydrogen-bonded to N2 again as the acceptor. In this case the distance is shorter (2.59 Å), and the interaction between N2 and O8 is much stronger. The angle C3–N2–C7 is 118.2(6)°, close to 120°. However, two hydrogen atoms were localized on this nitrogen atom; this shows the protonated nature of this nitrogen atom and the tetrahedral symmetry. This nitrogen is also hydrogen-bonded to one of the two water molecules (O9w) at a distance of 2.91 Å through H27 with an angle of 152.8°.

The third nitrogen atom is bonded to only one hydrogen atom, the C5–N3–C6 angle is 117.72(7)°; close to 120°. This atom is non-protonated. However it is hydrogen-bonded to O11 through H18. O11 (oxygen from phosphonate group P4), is also protonated (H24), however this proton does not participate into the hydrogen bonding network, O11 is acting as an acceptor in this case and is also hydrogen-bonded with N4 (donor), which is protonated. Two hydrogen atoms (H20 and H28) were localized on this atom and the angle C4–N4–C8 is 108.2(6)° very close to the tetrahedral angle. H28 points towards O10w with an angle of 125.7° and the distance N4···O10w is 2.84 Å. H20 points towards O11 with an angle of 110.8° and the distance N4···O11 is 3.09 Å.

The two water molecules are also hydrogen-bonded to the two chlorine atoms. These two molecules are then stabilized by their multiple hydrogen bonding, which explains why they are thermally removed between 100 °C and 200 °C (thermogravimetric analyses, Figure 1). This loss of water is accompanied by structure collapse.

The distribution of protons from the phosphonate groups to three of the four nitrogen atoms (N1, N2, N4) requires that the two phosphonic acids have different negative charges. The P1, P4 ligand has both nitrogen atoms

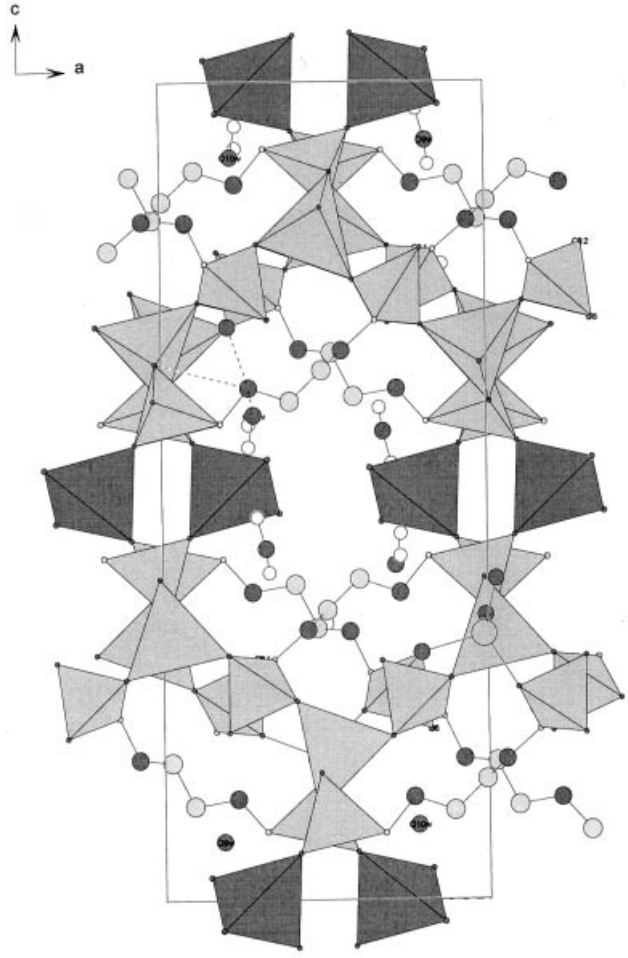

Figure 4. Tetrahedral representation of the structure in the *a,c* plane. The large gray tetraedra represent $[Zn1O_4]^{6-}$ and $[Zn3O_4]^{6-}$; darker gray tetraedra $[Zn2Cl_2O_2]^{4-}$ and small gray tetraedra the phosphonate groups.

protonated as well as O11; therefore it has a charge of minus one. The P2, P3 ligand has only N4 protonated and a charge of minus three.

Spectroscopic Studies

FTIR: The crystal structure of H_4L[13] shows both nitrogen atoms to be protonated. The IR spectrum of this zwitterion is shown in Figure 5a, together with that of the zinc compound. The range of PO vibrations in the IR spectrum of H_4L supports the betaine structure. The spectrum exhibits three strong bands at 1156, 1029 and 939 cm^{-1}, assigned respectively to $\nu_{as}(PO_2)$, $\nu_s(PO_2)$and ν(POH), indicating clearly the presence of PO_3H groups. [10] Furthermore, all the PO bands are low-frequency shifted due to the strong intra- and intermolecular hydrogen bonds with lattice water molecules and NH_2^+ groups. The NH_2^+ bands are expected to give two bands between 3000 and 2700 cm^{-1}, which are usually broad, unresolved and extended to 2273 cm^{-1}. Indeed, the IR spectrum of H_4L shows a broad and shallow band at 2800–2400 cm^{-1} revealing the presence of the protonated NH groups.

The IR spectrum of zinc phosphonate is complicated (see b in Figure 5). Phosphonic groups are coordinated with metal and the ν(P–OH) band observed in H_4L disappears upon coordination. The other vibrations associated with the POH group [ν(PO–H), 2δ(POH)] can still be detected with a decrease of their intensity. Two new sharp bands at 1130 and 1107 cm^{-1} can principally be assigned to both $\nu(PO_2)$ and $\nu(PO_3)$ vibrations. The zwitterionic structure of the compound could also be observed, in the region 3400–2500 cm^{-1} of the spectrum. In fact the NH stretching vibrations band is high-frequency shifted with much higher $\Delta\nu$ (91 cm^{-1}) value than the CdL_2H_2O[9] compound. At the same time, the $\nu(NH_2^+)$ band belonging to acid H_4L is still present in the spectrum. Only a slight decrease in the intensity of this band was observed. The NH_2^+ bending band does not appear in the spectrum. This spectrum can be interpreted in terms of partial protonation of nitrogen atoms and presence of both POH and PO groups, which is in accordance with the structure data.

Conclusions

It is interesting to note that while both the zinc and the cadmium complexes with the ligand H_4L were prepared in a very similar fashion, the stoichiometry and hence the structures are completely different. The Cd complex is octahedrally coordinated[9] by two Cl, two phosphonate oxygen atoms and two water molecules. The chloride ions bridge across two cadmiums while the phosphonate groups connect these dimers into double-stranded chains. In the process the double-stranded chains are crosslinked into layers that are hydrogen-bonded to each other. Both IR and NMR showed that the nitrogen atoms are protonated. In the zinc structure the differences are striking. The Zn atoms are four coordinate in which the chloride ions reside on a single zinc atom and do not bridge across metal atoms. The distribution of the ligand protons is also different, three of the nitrogen atoms are protonated but N3 is not and water molecules are not bonded to zinc. Therefore a moreaccurate formula is $Zn_3Cl_2(O_3PCH_2NH_2^+CH_2CH_2\text{-}NH_2^+CH_2PO_3)(HO_3PCH_2NHCH_2CH_2NH_2^+CH_2PO_3)\cdot 2H_2O$. These studies show that the H_4L ligand can adjust its coordination and behavior in several different as not yet totally explored ways.

Experimental Section

Materials and Methods: All chemicals were obtained from commercial sources and used without further purification. The ethylenediamine-*N,N'*-bis(methylenephosphonic acid) (H_4L) was synthesized as described previously.[9]

Synthesis of $Zn_3Cl_2(H_2L)_2\cdot 2H_2O$: A solution of zinc chloride (EM Science, 10.6 mmol, 15 mL) in water was added to a suspension of H_4L (5.3 mmol, 15 mL) with brisk stirring. The pH was adjusted to 2 with hydrochloric acid (5 M) and the mixture was transferred to a Teflon-lined pressure vessel and kept at 150 °C for 5 days. The lower pH aided the formation of the crystalline powder. The

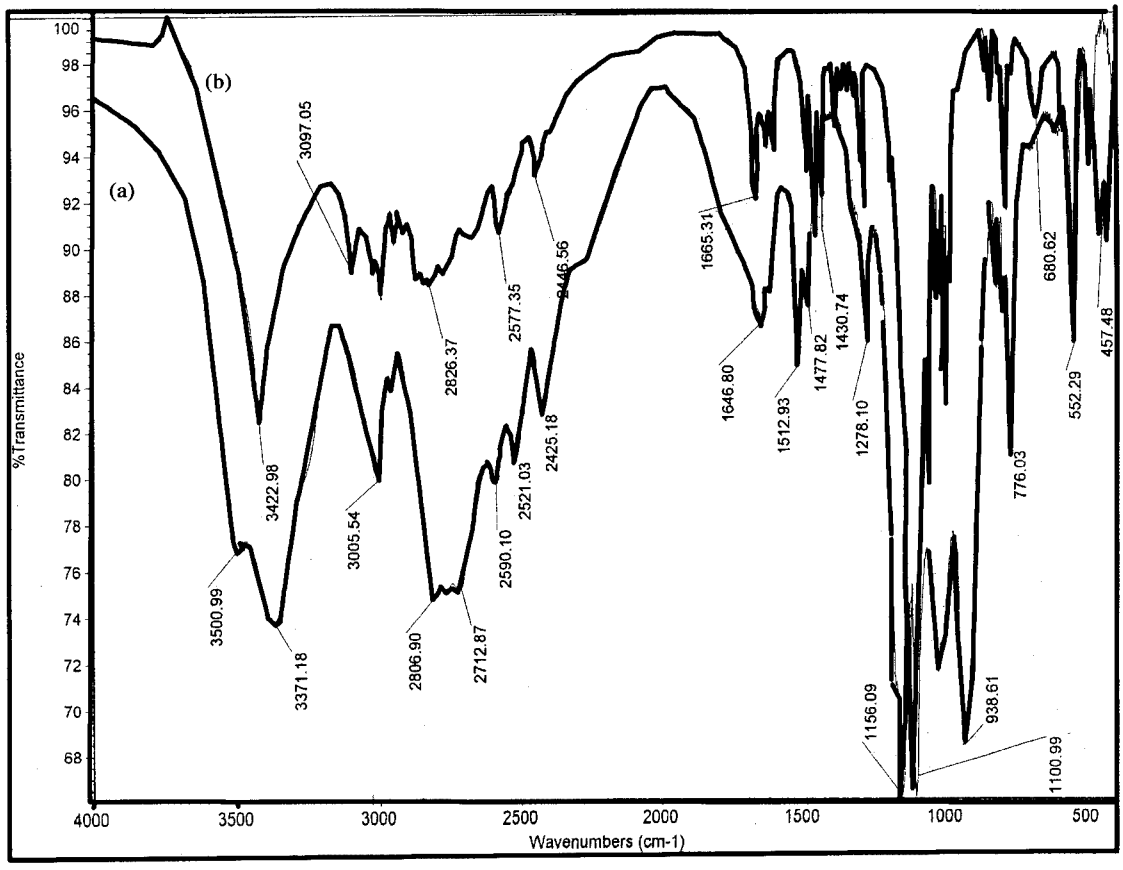

Figure 5. IR spectra of $Zn_3Cl_2L_2{\cdot}2H_2O$ (b) compared to aminophosphonic acid H_4L (a).

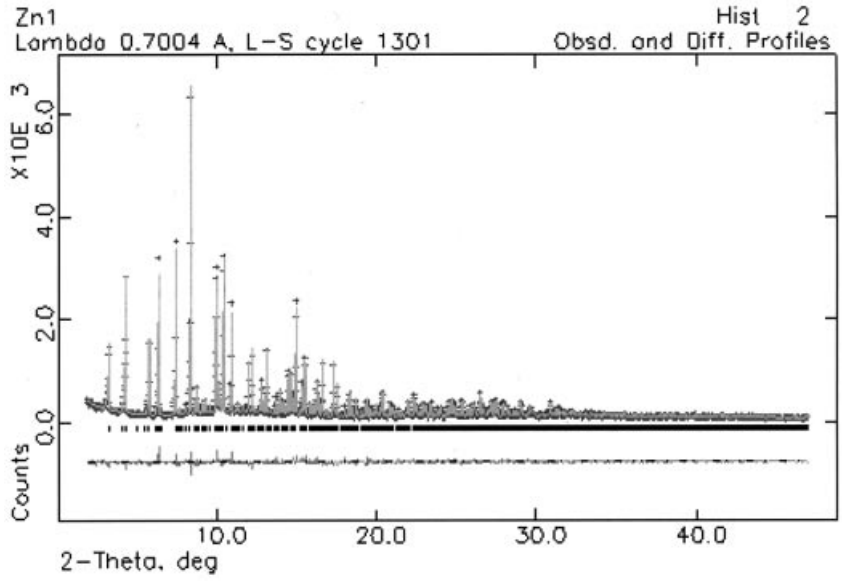

Figure 6. Observed (+), calculated (–) and difference profiles for the Rietveld refinement of $Zn_3Cl_2L_2{\cdot}2H_2O$.

resulting solid compound was filtered, washed with water and dried at 60 °C (0.96 g, 56%). $C_8H_{28}Cl_2N_4O_{14}P_4Zn_3$ (793.28): calcd. C 12.08, H 3.55, N 7.04, P 15.58, Cl 8.92, Zn 24.67; found C 12.27, H 3.72, N 7.12, P 15.13, Cl 8.67, Zn 24.16. IR: $\tilde{\nu}$ = ν(OH) 3423 cm^{-1} (ms) and $\nu(NH_2^+)$; ν(NH) 3097 cm^{-1} (mw), 3020, (mw), 2996, (mw), $\nu(CH_2)$, around 2826 cm^{-1} (bw); ν(PO–H), 2δ(POH) 2800–2400 cm^{-1} (mw); δ(HOH) 1665, 1623 cm^{-1} (w); δ NH_2^+) 1595 cm^{-1}; $\delta(CH_2)$ 1481–1384 cm^{-1} (w); $\omega(CH_2)$ 1288 cm^{-1} (mw); ν(PO) 1130 cm^{-1} (s), 1107 cm^{-1} (s).

The IR spectra were recorded with a Nicolet Nexus 470 FTIR spectrometer with spectral resolution of 2 cm^{-1} in KBr pellets. Thermo-

gravimetric analysis was carried out with a DuPont TGA 951 instrument at a heating rate of 10 °C/min under compressed air. The obtained compounds were characterized by their X-ray powder data collected with either a Rigaku 5000 computer-automated diffractometer with rotating anode or a Bruker advance diffractometer by the step scan method with Cu-K_α radiation (λ = 1.5418 Å).

Analytical Results: Zinc and phosphorus analysis was carried out in-house with a Direct Current Plasma (DCP) spectrometer. A weighed portion of the sample was dissolved in 1 mL of 48% HF and then diluted to 200 mL. Aliquots were then removed and diluted to a composition falling well within the standard curves for Zn and P, respectively. Alternatively these elements were also determined using a Cameca 5 × 50 electron microprobe at an accelerating voltage of 15 kV and operating with a beam current of 20 mA using a wavelength-dispersive spectrometer (WDS). C,H,N analyses were performed by Galbraith laboratories.

In-house X-ray Diffraction

Parameters Determination (high-resolution data): An X-ray powder diffraction pattern was recorded using a Bruker D8 advance, high resolution X-ray diffractometer with Bragg–Brentano θ−2θ geometry (40 kV and 50 mA), using a Ge monochromator with Cu-$K_{\alpha 1}$ radiation (λ = 1.54056 Å). The data were recorded between 5 and 95° in 2θ, with a step size of 0.01° and a count time of 30 s per step. The sample was packed in a flat plastic holder, and was allowed to rotate at 15.00 RPM during the data collection.

Structure Solving and Refinement (intensity data): X-ray powder diffraction patterns were recorded using a Bruker D8 diffractometer with Bragg–Brentano θ–2θ geometry (40 kV and 50 mA), using a graphite monochromator. The data were recorded between 5 and 60° in 2θ, with a step size of 0.01° and a count time of 20 s per step, and 50 to 100° in 2θ, with a step size of 0.01° and a count time of 25 s per step. The sample was packed in a flat plastic holder.

Table 1. Crystal data.

Empirical formula	$C_8H_{26}Cl_2N_4O_{14}P_4Zn_3$
Formula mass	793.28
Crystal system	monoclinic
Space group	$P2_1/n$ (no. 14)
Unit cell dimensions	a = 9.94316(4) Å
	b = 10.44577(5) Å
	c = 24.3240(1) Å
	β = 90.003(1) °
Cell volume	2526.39(2) Å^3
Z	4
Density, calculated	2.017 g/cm^3
Rwp[a], Rp[b], R_f	0.0574, 0.07454, 0.0455

[a] $Rwp = (\Sigma\, w(I_o - I_c)^2/\Sigma w I_o^2)^{0.5}$ (w = weighting factor). [b] $Rp = \Sigma \mid I_o - I_c \mid/\Sigma\, I_o$. [c] $R_f = \Sigma\, |F_o - SF_c|/\Sigma\, |F_o|$ (S = scale factor)

Table 2. Atomic coordinates and isotropic displacement parameters (in Å^2) for non-hydrogen atoms.

Atom	Wyck.	x	y	z	U_{iso}
ZN1	4e	0.4880(3)	0.0411(3)	0.8230(1)	0.0106(2)
ZN2	4e	0.6967(2)	0.2469(8)	0.0004(3)	0.0106(2)
ZN3	4e	0.9811(3)	0.0406(3)	0.6738(1)	0.0106(2)
Cl1	4e	0.8248(5)	0.4023(5)	0.03790(3)	0.032(1)
Cl2	4e	0.1399(5)	0.9024(5)	0.0278(3)	0.032(1)
P1	4e	0.4986(5)	0.2823(5)	0.8969(2)	0.0228(6)
P2	4e	0.4894(5)	0.2119(5)	0.1004(2)	0.0228(6)
P3	4e	0.7762(5)	0.0028(5)	0.2464(2)	0.0228(6)
P4	4e	0.2193(6)	0.4946(5)	0.2428(2)	0.0228(6)
O1	4e	0.5181(10)	0.3575(6)	0.8452(3)	0.0174(8)
O2	4e	0.1153(7)	0.0859(8)	0.701(3)	0.0174(8)
O3	4e	0.5100(13)	0.3552(6)	0.1075(3)	0.0174(8)
O4	4e	0.5842(7)	0.3367(8)	0.9434(3)	0.0174(8)
O5	4e	0.5256(13)	0.1407(6)	0.8904(3)	0.0174(8)
O6	4e	0.5942(8)	0.1646(8)	0.0590(3)	0.0174(8)
O7	4e	0.4932(13)	–0.1402(6)	0.8465 (3)	0.0174(8)
O8	4e	0.8269(8)	0.5354(10)	0.2084(3)	0.0174(8)
O9w	4e	0.1814(11)	0.5132(13)	0.0714(4)	0.0174(8)
O10w	4e	0.7824(12)	–0.0106(9)	0.0913(4)	0.0174(8)
O11	4e	0.1991(9)	0.0162(11)	0.2046(3)	0.0174(8)
O12	4e	0.7045(7)	0.9338(10)	0.1994(3)	0.0174(8)
O13	4e	0.2992(7)	0.4161(9)	0.2015(3)	0.0174(8)
O14	4e	0.4078(7)	0.9155(10)	0.2428(3)	0.0174(8)
N1	4e	0.2312(5)	0.2871(7)	0.8750(3)	0.032(2)
N2	4e	0.0550(7)	0.6144(6)	0.1702(3)	0.032(2)
N3	4e	0.2247(5)	0.2188(10)	0.1236(3)	0.032(2)
N4	4e	0.9241(6)	0.1320(6)	0.1722(3)	0.032(2)
C1	4e	0.3942(6)	–0.1736(7)	0.6084(3)	0.053(3)
C2	4e	0.3202(6)	0.3068(8)	0.9189(3)	0.053(3)
C3	4e	0.4938(7)	–0.2204(6)	0.6463(3)	0.053(3)
C4	4e	−0.0239(6)	–0.2210(6)	0.8320(3)	0.053(3)
C5	4e	0.0922(6)	0.1976(8)	0.1147(3)	0.053(3)
C6	4e	0.3147(7)	0.1787(8)	0.0833(3)	0.053(3)
C7	4e	0.1595(8)	0.6351(7)	0.2066(3)	0.053(3)
C8	4e	0.8629(9)	0.1461(7)	0.2231(3)	0.053(3)

[a] $U_{iso} = B_{iso}/8\Pi^2$

Synchrotron Powder X-ray Diffraction: Powder X-ray diffraction data were collected at ambient temperature on beamline X3B1 of the National Synchrotron Light Source at Brookhaven National Laboratory. X-rays of wavelength 0.70045(1) Å was selected by a double crystal Si(111) monochromator. The sample was sealed in a capillary, which was continuously rotated during data collection. The data collection time increased from 1 s per point at 2 degrees 2θ to 5.7 s at 46.997°, with a step size of 0.003°. The diffracted X-rays are selected by a Ge (111) analyzer crystal on a detector arm, and detected using a commercial NaI scintillation counter; the measured X-ray counts are normalized to the signal from an ionization chamber between the monochromator and the sample in order to correct for decay and fluctuations of the incident beam intensity.

Structure Determination: A first determination of cell parameters was made using Treor90 program[11] on the in-house data. The indexing yielded the cell dimensions: a = 9.942(1), b = 10.445(1), c = 23.317(4) Å, β = 90.001(1)° and V = 2526.46(2) Å^3 as the best solution [M (20) = 51]. The β angle is very close to 90°, the cell parameters are then reflective of an orthorhombic symmetry. The analyses of the systematic absences are consistent with the space group $Pna2_1$. However, we were not able to solve the structure in this space group or in any orthorhombic space group which could reproduce the powder pattern. We considered then a small distortion of the β angle to reflect a monoclinic distortion. The analyses of the systematic absences were consistent with the space group $P2_1/n$. The first attempt to solve this structure in the in-house data, using EXPO,[12] allowed us to localize a few of the atoms. Respectively, three zinc atoms, three of the four phosphorus atoms, and the two chlorine atoms. The calculation of successive Fourier difference maps followed by Rietveld refinement (using the program GSAS[13]) allowed us to locate most of the oxygen atoms and one ligand, but we were not able to go further. For this reason, we recorded a synchrotron data set, which allowed us to localize most of the atoms by direct methods and the rest of them by Fourier difference maps.

The refinement strategy consisted in a first step of a Lebail method refinement for the background (using 12 terms of a Chebychev function), zero shift, cell parameters and peak profile function, considering a dummy hydrogen atom and maintaining a scale factor constant and equal to 1. Once these parameters were satisfactory (Rp = 0.07), they were fixed, the known atoms were entered into the program and the scale factor refined. By successive refinement and Fourier difference maps, all the atoms were located. The following bond constraints were applied: Zn–O (2.0 Å), Zn–Cl (2.6 Å), P–O (1.52Å), P–C (1.80 Å), C–N (1.34 Å), C–C (1.54 Å) and C–H (1 Å) prior to position refinement of the atoms. The bond angles around the phosphorus atom were constrained to idealized tetrahedral angles by applying constraints to the non-bonded O···O (2.5 Å) and O···C (2.7 Å) distances, and tetrahedral angles around the carbon atom. The position for the hydrogen atoms were calculated for the carbon atoms and a final Fourier difference allowed us to localize the remaining hydrogen atoms. The carbon hydrogen atom position were refined but not the nitrogen hydrogen atoms or the water hydrogen. The constraint parameter was first fixed to 500 and then lowered to 100 in the last cycle of the refinement. The atomic positions were refined first, then the temperature factors, and finally all the parameters were refined simultaneously. The last set of refinement yielded a value of R_p = 0.0567, R_{wp} = 0.0733 and R_F = 0.0424.

Figure 6 shows the observed powder pattern, the calculated and the difference curve after the last refinement, from the synchrotron

Table 3. Selected geometric parameters, distances and angles [Å, °]

ZN1–O5	1.978(8)	O5–ZN1–O7	104.9(3)
ZN1–O7	1.980(7)	O5–ZN1–O12	109.7(4)
ZN1–O12	2.006(8)	O5–ZN1–O14	117.1(4)
ZN1–O14	1.958(8)	O7–ZN1–O12	103.2(5)
		O7–ZN1–O14	116.4(4)
		O12–ZN1–O14	104.7(3)
ZN2–Cl1	2.256(9)	Cl1–ZN2–O4	104.9(5)
ZN2–O4	2.012(9)	Cl1–ZN2–O6	108.4(4)
ZN2–O6	1.953(9)	Cl1–ZN2–Cl2	101.8(2)
ZN2–Cl2	2.353(8)	O4–ZN2–O6	114.7(3)
		O4–ZN2–Cl2	119.5(4)
		O6–ZN2–Cl2	106.3(5)
ZN3–O1	1.968(7)	O1–ZN3–O2	113.3(4)
ZN3–O2	1.970(8)	O1–ZN3–O3	110.1(3)
ZN3–O3	1.968(8)	O1–ZN3–O13	107.8(4)
ZN3–O13	1.982(8)	O2–ZN3–O3	109.8(4)
		O2–ZN3–O13	109.1(3)
		O3–ZN3–O13	106.6(4)
P1–O1	1.494(8)	O1–P1–C2	106.7(5)
P1–C2	1.876(8)	O1–P1–O4	110.2(5)
P1–O4	1.521(8)	O1–P1–O5	113.8(5)
P1–O5	1.512(8)	C2–P1–O4	105.3(4)
		C2–P1–O5	109.1(6)
		O4–P1–O5	110.3(6)
P2–O3	1.522(8)	O3–P2–O6	107.5(6)
P2–O6	1.530(9)	O3–P2–O7	112.2(5)
P2–O7	1.502(8)	O3–P2–C6	110.0(6)
P2–C6	1.819(8)	O6–P2–O7	109.0(6)
		O6–P2–C6	116.0(5)
		O7–P2–C6	102.2(6)
P3–O2	1.533(9)	O2–P3–O8	109.5(5)
P3–O8	1.542(9)	O2–P3–O12	108.8(5)
P3–O12	1.528(9)	O2–P3–C8	106.3(5)
P3–C8	1.817(9)	O8–P3–O12	109.2(5)
		O8–P3–C8	110.8(5)
		O12–P3–C8	112.2(5)
P4–O11	1.533(9)	O11–P4–C7	117.4(6)
P4–O13	1.521(9)	O11–P4–O13	110.8(6)
P4–O14	1.550(9)	O11–P4–O14	108.7(6)
P4–C7	1.812(9)	C7–P4–O13	106.7(5)
		C7–P4–O14	105.9(5)
		O13–P4–O14	106.8(5)
C1–C3	1.440(9)	C3–C1–N1	109.5(6)
C1–N1	1.373(8)		
C2–N1	1.403(9)	P1–C2–N1	111.2(5)
C3–N2	1.391(9)	C1–C3–N2	107.4(6)
C4–C5	1.484(9)	C5–C4–N4	106.6(6)
C4–N4	1.364(9)		
C5–N3	1.353(8)	C4–C5–N3	106.2(6)
C6–P2	1.819(8)	P2–C6–N3	113.3(6)
C6–N3	1.393(10)		
C7–N2	1.381(10)	N2–C7–P4	115.6(6)
C8–N4	1.388(9)	P3–C8–N4	113.5(5)
N1–C1	1.373(8)	C1–N1–C2	107.7(6)
N1–C2	1.403(9)	C1–N1–H21	113.4(9)
N1–H21	1.015(11)	C1–N1–H22	112.2(10
N1–H22	1.018(11)	C2–N1–H21	111.2(9)
		C2–N1–H22	110.0(10)
		H2–N1–H21	102.3(11)
N2–C3	1.391(9)	C3–N2–C7	118.2(6)
N2–C7	1.381(10)	C3–N2–H17	109.3(8)
N2–H17	1.041(12)	C3–N2–H27	108.7(8)
N2–H27	1.036(11)	C7–N2–H17	109.6(9)
		C7–N2–H27	110.0(9)
		H17–N2–H27	99.4(10)
N3–C5	1.353(8)	C5–N3–C6	117.7(7)
N3–C6	1.393(10)	C5–N3–H18	115.7(12)
N3–H18	1.000(13)	C6–N3–H18	114.3(15)
N4–C4	1.364(9)	C4–N4–C8	108.2(6)
N4–C8	1.388(9)	C4–N4–H20	112.9(9)
N4–H20	1.021(10)	C4–N4–H28	111.5(9)
N4–H28	1.021(11)	C8–N4–H20	110.7(10)
		C8–N4–H28	111.2(8)
		H20–N4–H28	102.3(12)
O9w–H14	0.96(11)	H14–O9w–H19	123.(7)
O9w–H19	1.004(21)		
O10w–H15	1.014(21)	H15–O10w–H16	93.0(32)
O10w–H16	1.005(20)		
O11–P4	1.533(9)	P4–O11–H24	93.(7)
O11–H24	1.05(10)		

data set. Table 1 presents the crystallographic data. The atomic positions, the bond lengths and angles are represented in Table 2 and Table 3, respectively. CCDC-249450 contains the supplementary crystallographic data for this paper. This data can be obtained free of charge via www.ccdc.cam.ac.uk/data_request/cif.

Acknowledgments

This study was supported with funds provided by NSF Grant No. DMR 0332453, for which grateful acknowledgement is made. We thank Nicholas A. Spurr for the DCP analysis, Dr. Guillemette (Geology department, Texas A&M University) for the microprobe analysis and Dr. P. Stephens (Physics and Astronomy Department, SUNY Stony Brook) for his assistance with synchrotron X-ray data collection. Research carried out in part at the National Synchrotron Light Source at Brookhaven National Laboratory, which is supported by the US Department of Energy, Division of Materials Sciences and Division of Chemical Sciences. The SUNY X3 beamline at NSLS is supported by the Division of Basic Energy Sciences of the US Department of Energy under Grant No. DE-FG02-86ER45231.

[1] a) A. Clearfield, *Curr. Opin. Solid State Mater. Sci.* **1996**, *1*, 268; b) A. Clearfield, *Curr. Opin. Solid State Mater. Sci.* **2002**, *6*, 495; c) A. Clearfield, in *Progress in Inorganic Chemistry* (Ed.: K. D. Karlin), John Wiley & Sons, New York, **1998**, 371; d) C. V. K. Sharma, A. Clearfield, *J. Am. Chem. Soc.* **2000**, *122*, 4394–4402; e) C. V. K. Sharma, C. V. Hesseheimer, J. Amelia, A. Clearfield, *Polyhedron* **2001**, *20*, 2095–2104; f) A. Clearfield, C. V. K. Sharma, B. Zhang, *Chem. Mater.* **2001**, *13*, 3099–3112; g) A. Clearfield, Z. J. Wang, *J. Chem. Soc. Dalton Trans.* **2002**, *23*, 4457–4463.

[2] a) G. Alberti, in *Comprehensive Supramolecular Chemistry* (Eds.: G. Alberti, T. Bein), Elsevier Sci. Ltd., Oxford, **1996**, vol. 7, p. 151; b) G. Alberti, E. Brunet, C. Dionigi, O. Juanes, M. J. De la Mata, J. C. Rodriguez-Ubis, R. Vivani, *Angew. Chem. Int. Ed.* **1999**, *38*, 3351–3353; c) G. Alberti, E. Giontella, S. Murcia-Mascaros, *Inorg. Chem.* **1997**, *36*, 2844–2849.

[3] a) B. Bujoli, P. Palvadeau, J. Rouxel, *Chem. Mater.* **1990**, *2*, 582–489 .; b) J. Le Bideau, C. Payen, P. Palvadeau, B. Bujoli, *Inorg. Chem.* **1994**, *33*, 4885–4890; c) F. Fredoueil, D. Massiot, D. M. Poojary, M. Bujoli-Doeuff, A. Clearfield, B. Bujoli, *Chem. Commun.* **1998**, *2*, 175–176; d) F. Odobel, B. Bujoli, D. Massiot, *Chem. Mater.* **2001**, *13*, 163–173.

[4] a) D. Riou, C. Serre, G. Ferey, *J. Solid State Chem.* **1998**, *141*, 89–93; b) D. Riou, G. Ferey, *J. Mater. Chem.* **1998**, *8*, 2773–2735; c) D. Riou, C. Serre, J. Provost, G. Ferey, *J. Solid State Chem.* **2000**, *155*, 238–242; d) F. Serpaggi, G. Ferey, *J. Mater. Chem.* **1998**, *8*, 2749–2755; e) B. A. Adair, N. Guillou, A. Marisol, G. Ferey, A. K. Cheetam, *J. Solid State Chem* .**2001**, *162*, 347–353.

[5] a) A. Clearfield, Z. J. Wang, *J. Chem. Soc. Dalton Trans. Chem. Soc. Dalton Trans.* **2002**, 4457–4463; b) C. Y. Yang, Ph. D. Dissertation, Texas A&M University, Dec. **1986**; c) A. Clearfield, *Chem. Mater.* **1998**, *10*, 2801–2810.

[6] D. M. Poojary, B. Zhang, A. Clearfield, *J. Am. Chem. Soc.* **1997**, *119*, 12550–12559.

[7] D. I. Arnold, X. Ouyang, A. Clearfield, *Chem. Mater.* **2002**, *14*, 2020–2027.

[8] C. Y Ortiz-Avila, C. Bhardwaj, A. Clearfield, *Inorg. Chem.* **1994**, *33*, 2499–2500.

[9] E. V. Bakhmoutova-Albert, N. Bestaoui, V. Bakhmutov, A. Clearfield, A. V. Rodriguez, R. Llavona, *Inorg. Chem.* **2004**, *43*, 1264–1272.

[10] L. M. Shkol'nikova, G. V. Polyanchuck, V. E. Zadovnik, M. V. Rudomino, S. A. Pisareva, N. M. Dyatlova, B. V. Zdanov, I. Polyakova, *J. Struct. Chem.* **1987**, *28*, 104.

[11] P. E Werner, L. Eriksson, M. J. Westdahl, *Appl. Crystallogr.* **1985**, *18*, 367–370.

[12] "EXTRA: A program for extracting Structure-Factor Amplitudes from Powder Diffraction Data" A. Altamore, M. C. Burla., G. Cascarano, C. Giacovazzo, A. Guagliardi, A. G.G moliterni, G. Polidori, *J. Appl. Crystallogr.* **1995**, *28*, 842–846.

[13] a) A. Larson, R. B. von Dreele, GSAS: Generalized Structure Analysis System; Los Alamos National Laboratory, NM, **1986**; b) A. Z. March, *Kristallogr.* **1986**, *81*, 285; c) W. A. Dollase, *J. Appl. Crystallogr.* **1986**, *19*, 267–272..

Received: October 18, 2004

